The 7 June 2007 mb_{Lg} 4.2 Escopete Earthquake: An Event with Significant Ground Motion in a Stable Zone (Central Iberian Peninsula)

E. Carreño,[1] B. Benito,[2] J. M. Martínez Solares,[1] L. Cabañas,[1] J. Giner,[5] P. Murphy,[4] C. López,[1] C. Del Fresno,[3,1] J. M. Alcalde,[1] J. M. Gaspar-Escribano,[2] R. Antón,[1] J. Martínez-Díaz,[5] S. Cesca,[7] A. Izquierdo,[1] J. G. Sánchez Cabañero,[6] and P. Expósito[1]

INTRODUCTION

An earthquake occurred on 7 June 2007 at 01h:42m:09.5s (UTC) with geographical coordinates 40°.41N, 2°.98W and magnitude $mb_{Lg} = 4.2$ according to the Seismic national network (RSN) of Madrid's Instituto Geográfico Nacional (IGN). The epicenter was located close to the town of Escopete, where the earthquake was felt with intensity IV, waking up inhabitants and causing widespread alarm. Historically, rare but similar events have been felt in the area, near the towns of Pastrana (1922) and Duron (1982). Nevertheless, this part of Iberia experiences very low seismic activity. The earthquake with the largest magnitude recorded to date by the RSN since the mid-1920s was 4.1. Due to low seismicity values, the hazard map of the Norma de la Construcción Sismorresistente Española (Spanish seismic building code; NCSE-02) establishes a basic acceleration value of less than 0.04 g, which is the threshold value for the application of the earthquake-resistant building code. However, this value was exceeded in strong-motion recordings during the 2007 event.

An important consideration is the existence of two nuclear power plants in the Guadalajara administrative province: José Cabrera and Trillo. Strong-motion instruments at the José Cabrera nuclear power plant (JCNPP) recorded a peak ground acceleration (PGA) value of 0.07g. This is the first acceleration recording made from central Iberia and also one of the highest values read from instruments to date for the whole of the Iberian peninsula.

1. Instituto Geográfico Nacional, Madrid, Spain
2. Escuela Técnica Superior de Ingenieros en Topografía, Geodesia y Cartografía, Universidad Politécnica de Madrid
3. Departamento de Geofísica y Meteorología, Universidad Complutense, Madrid
4. Architect, Madrid, Spain
5. Facultad de Ciencias Geológicas, Universidad Complutense de Madrid
6. Consejo de Seguridad Nuclear, Madrid, Spain
7. Seismologisches Zentral Observatorium BGR, Erlangen, Germany

This paper presents an overview of the results of our multidisciplinary analysis of the earthquake, which we researched in terms of its regional and local tectonic setting, local seismicity, focal mechanics, strong-motion records, and macroseismic effects.

SEISMICITY AND TECTONICS OF THE REGION

The study region for this earthquake covers an area of 100 × 100 km and is located 50 km east of Madrid in the central part of Iberia. The area is characterized by low seismicity. Incorporating both historical and instrumental data from 1755 to 2007, the complete earthquake dataset for this zone includes only 78 events (Martínez Solares and Mezcua 2002; Instituto Geográfico Nacional 2007). The seismotectonic map of the area is shown in Figure 1. Earthquakes show continuity in time only after 1980, following the expansion of the Spanish seismic network. The maximum intensity reported for the area is V, and the highest magnitude recording is 4.1 corresponding to the 1980–2007 instrumental period. Only three events have met these threshold values. The first one, in 1922, was very similar to the 2007 event under study, with an observed intensity of V on the European Macroseismic Scale (EMS) and an epicenter close to Pastrana and Escopete. Two other events of magnitude 4.1 occurred in the area in 1979 and 1982. The instrumental seismicity is shallow and most events have focal depths of less than 10 km.

We used a Gutenberg-Richter relation correlating the magnitude and frequency of earthquakes in the area to estimate the *b*-value, which describes the relative proportion of large to small earthquakes ($\log N = a - bM$). Using the least squares approach and considering catalog completeness above magnitude 3.0, we obtain $b = 0.7$. This low *b*-value may indicate that large events involving high stress drops are predominant in the region.

Compared to other regions of Iberia, the area has low activity and thus a low seismic hazard. The hazard map of the Spanish earthquake-resistant building code NCSE-02 (NCSE-02 2002), shown in Figure 2, indicates a value of less than 0.04 g

doi: 10.1785/gssrl.79.6.820

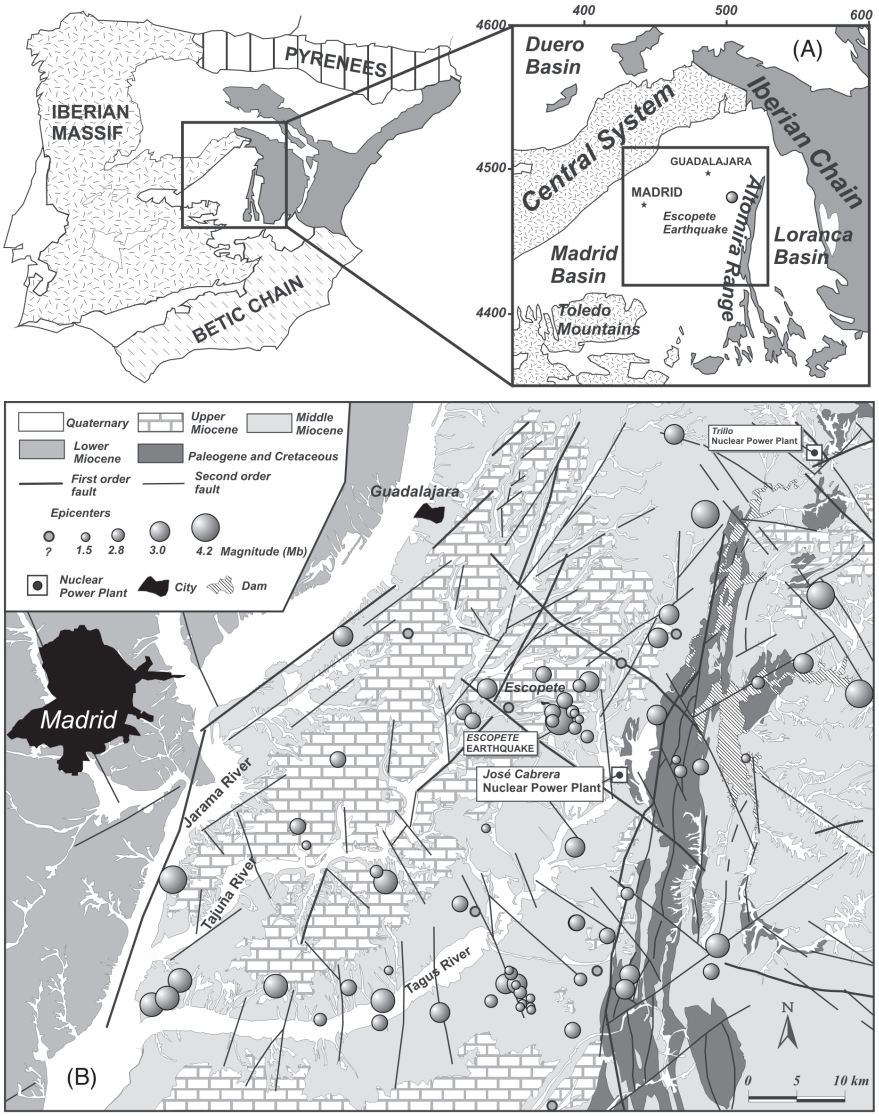

▲ **Figure 1.** (A) Location of the main geological units and the epicenter of the Escopete earthquake. (B) Geological map of the eastern Madrid basin. Major faults represented are taken from Proyecto Prior 2007. Gray circles are the epicenters of total seismic activity (period 1755–2007) from the IGN database.

for this area. The represented value is the NCSE-02 *basic acceleration*, a_b, corresponding to horizontal PGA in hard soil with a 10% exceedance probability for a 50-year exposure period. Expected a_b values for the entire central part of the Iberian peninsula (including Guadalajara province) are less than 0.04 g, which is also the minimum value represented in this hazard map. According to the NCSE-02, seismic design is not mandatory below this value; therefore, the code does not need to be applied in any part of the study area.

LOCAL SEISMOTECTONIC SETTING

The Escopete main event has been located using *P* and *S* phases from the closest stations (11 stations located within a radius of 250 km from the epicenter) with the same Earth velocity model used by the RSN of the IGN for regional seismicity, which gives us the hypocentral solution shown in Table 1.

A local Earth velocity model incorporating four horizontal layers with velocity gradients (Banda *et al.* 1981) has also been tested with the *P* phase only (Table 2). The new solution is similar to the previous one, with a slight reduction of the root mean square error. The estimated magnitude is set at $mb_{Lg} = 4.2$ with standard deviation $\sigma = 0.3$ in both cases.

Focal Mechanism

The focal mechanism of the Escopete earthquake has been calculated by moment tensor inversion, following the technique developed by Cesca *et al.* (2006). Fitted data correspond to body-wave digital records from seven IGN broadband stations located at regional distances (200–300 km) and with a good azimuthal coverage (azimuthal gap lower than 110°). We used the velocity model given in Table 2. We converted records to displacement time histories, removing the instrumental response and filtering high frequencies above 4 Hz. Data win-

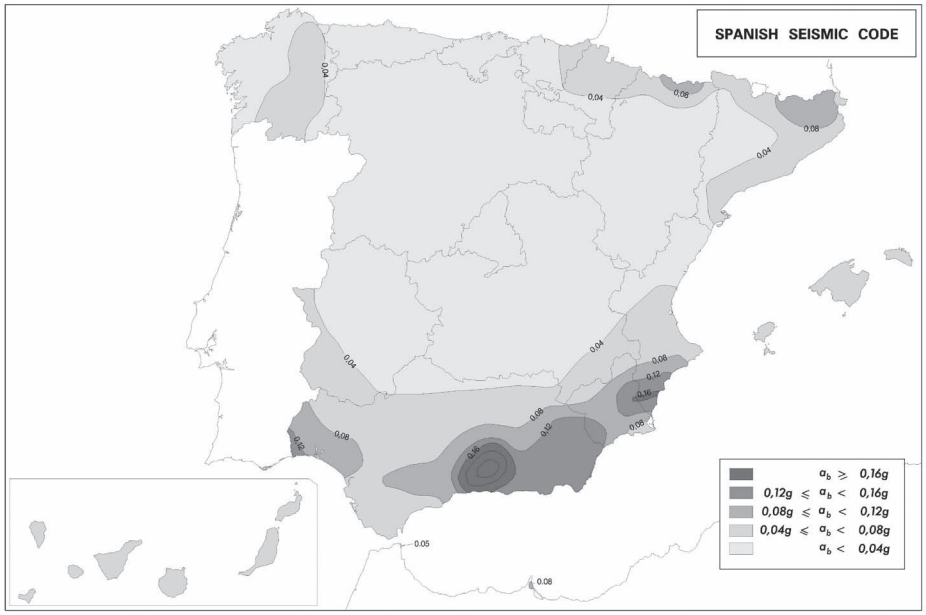

▲ **Figure 2.** Seismic hazard map of the Spanish seismic building code NCSE-02. Isolines represent "basic acceleration, a_b," which corresponds to expected PGA in hard soil for an exceedance of 10% in 50 years. The Guadalajara province is framed with a rectangle.

TABLE 1
Hypocentral Solutions Reached by Two Different Velocity Models

	IGN model	Local model (Banda *et al.*, 1981)
Date	07/06/2007	07/06/2007
Time (TUC)	01:42:09.8	01:42:09.5
Lat (°)	40.41 N	40.41N
Lon (°)	2.98 W	2.98W
Depth (km)	7.9	8.2
ERR_DEPTH (km)	3.5	5.6
SMIN (km)	4.4	4.3
SMAX (km)	6.6	7.0
Strike	153	154
RMS	0.69	0.57

SMIN : semiaxe minor of the error semielipse
SMAX: semiaxe major of the error semielipse
STRIKE : angle from the North of the major semiaxe

TABLE 2
Velocity Model for Central Iberia (Banda *et al.* 1981)

H (km)	Vp (km/s)	Vs(km/s)
2.5	3.30	2.50
4.4	6.05	4.34
	6.15	4.96
4.0	5.60	3.18
12	6.40	3.58
8.0	6.90	3.90
	6.80	

dows include *Pg* and *Pn* phases and have a time length of 2 s and 4 s, respectively, for displacement fits and for the calculation of spectral amplitudes. Inversions have been carried out for source depths between 2 and 20 km (with an increment of 2 km) in the frequency domain and following a mixed approach, fitting both amplitude spectra and displacements.

The results represented in Figure 3A show that the best moment tensor solution (MTS) is obtained by minimizing the amplitude spectra misfit, and the solution corresponds to a depth of 6 km with strike-slip mechanism (azimuth = 225°, dip = 75°, slip = 179°) and fault planes oriented NW-SSE and NE-SW. The moment tensor solution is dominated by the double-couple component, with a minor compensated linear vector dipole (CLVD) (3%). The scalar seismic moment is equal to 2.0×10^{14} Nm. This result has been supported by the mixed frequency-time inversion solution. The retrieved orientation of the fault planes is consistent with the solution obtained by fitting polarities of *P* waves, using 31 observations.

The apparent source time function of the main earthquake has been obtained using *S* waves of the three major aftershocks as empirical Green's functions. Due to bad signal-to-noise ratio in the aftershock seismograms, only one broad-band seismic station has been used (RETOR, az = 58°, Δ = 90 km). A high-pass filter with corner frequency of 1.2 Hz was necessary for aftershocks, and a cross correlation to align data was done prior to deconvolution. We used an iterative time-domain deconvolution technique implemented by Ligorría and Ammon (1999). A Gaussian low-pass filter, $\exp(\pi^2 f^2/a^2)$, that drops to amplitudes less than 0.1 at 12 Hz, was used to stabilize deconvolutions.

Results show a triangular apparent source time function of 0.5 s with a maximum seismic moment release during the first 0.2 s (Figure 3B). We obtained a scalar seismic moment of 3.1×10^{14} Nm using spectral analysis of *P* waves in nine

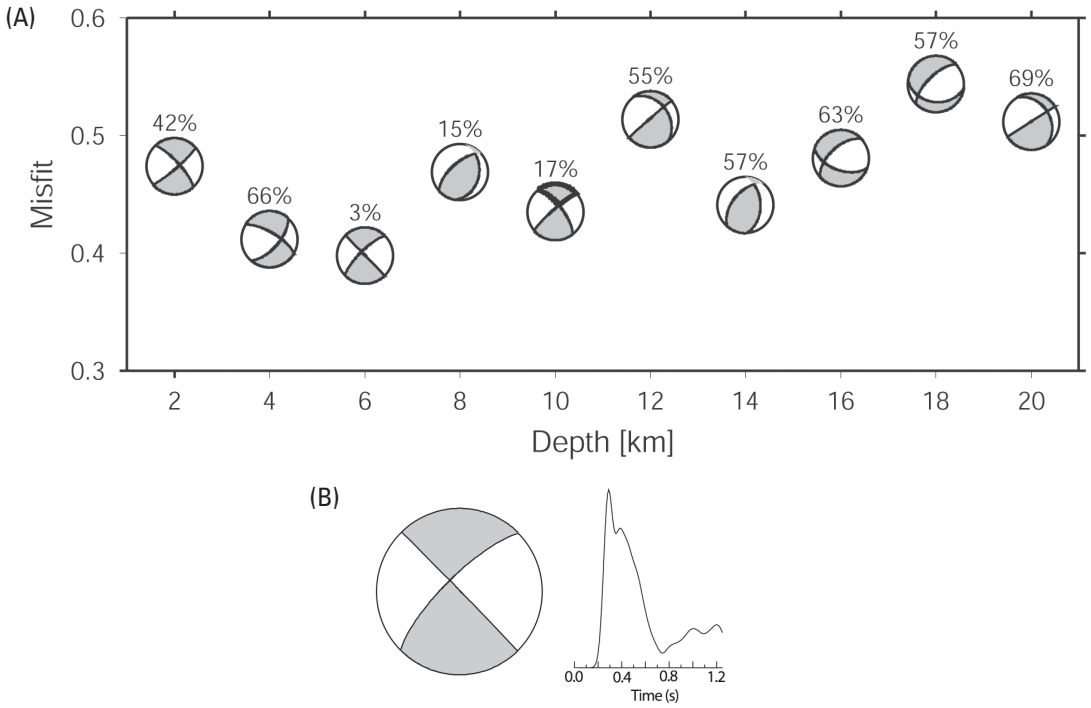

▲ **Figure 3.** (A) Results for the moment tensor inversion in the frequency domain. In the graphic the misfit versus depth is plotted, together with the double-couple solution. Percentages show the amount of CLVD for each inversion. The lower hemisphere of focal sphere has been represented. The black quadrants indicate compression and the white ones, dilations. (B) Focal mechanism for the moment tensor inversion with the lowest misfit and the apparent source time function obtained from the empirical Green's function method.

broadband stations with epicentral distances between 200 and 400 km. If Brune's model is considered, the results show a fracture with radius of 0.7 km.

Local Tectonic Setting

The study area is located in the eastern part of the Tagus basin. This basin is a triangular depression bounded by three intracratonic ranges with different tectonic styles: the Central System to the W-SW, the Iberian chain to the E-NE, and the Toledo Mountains to the south (Figure 1). The north-south-trending Altomira Range divides the Tagus basin into two parts: the western part, called the Madrid basin; and the eastern part, called the Loranca basin.

From a structural point of view the region has a Hercinian basement formed by metamorphic and granitic rocks. This basement is covered by a pretectonic layer of Mesozoic and Paleogene sediments. This cover is overlain by Neogene and Quaternary sediments. Miocene sedimentation is conditioned by tectonic activity along the basin border during the Middle to Late Miocene coinciding with the uplifting of the Central System (Calvo *et al.* 1996; De Vicente *et al.* 2007).

Previous studies in this area recognized the existence of significant tectonic activity from the Middle Miocene to the Quaternary (Giner *et al.* 1996). The major deformation structures are coherent with the regional horizontal stress shortening direction NW-SE (Herráiz *et al.* 2000), which is consistent with the current convergence direction between the Iberian and African plates (DeMets *et al.* 1990, 1994; Kiratzi and Papazachos 1995; McClusky *et al.* 2003).

Previous seismicity in the area shows scattered activity with some NW-SE alignments (Figure 4). Faults with neotectonic activity in the area are oriented NW-SE and NNE-SSW with normal and strike-slip components (Giner *et al.* 1996; De Vicente *et al.* 2007). Previous focal mechanism solutions in the area show reverse, normal, and strike-slip movements. The statistical analysis of the maximum horizontal shortening directions shows a predominant NW-SE direction. Reverse and strike-slip focal mechanisms are coherent with this direction and with the current regional stress regime. The maximum horizontal shortening NE-SW correspond with the extensional mechanisms interpreted by Giner *et al.* (1996) as related to a lithospheric flexure. This flexure would produce a extensional regime in shallower levels of the crust (Figure 4).

The focal mechanism of the Escopete earthquake presents two possible fault planes with strike-slip movement, a sinistral NW-SE plane and a dextral NE-SW plane. We can identify some NW-SE sinistral strike-slip faults with a small vertical component near the Escopete epicentral area, and these are coherent with one of the focal mechanism solutions.

MACROSEISMIC EFFECTS OF THE ESCOPETE EARTHQUAKE

The earthquake's epicenter was located in a sparsely populated area in the southern Alcarria region of the province of Guadalajara. This area is sparsely populated, with clusters of small towns separated by large stretches of open countryside. These conditions contrast with the densely populated Henares

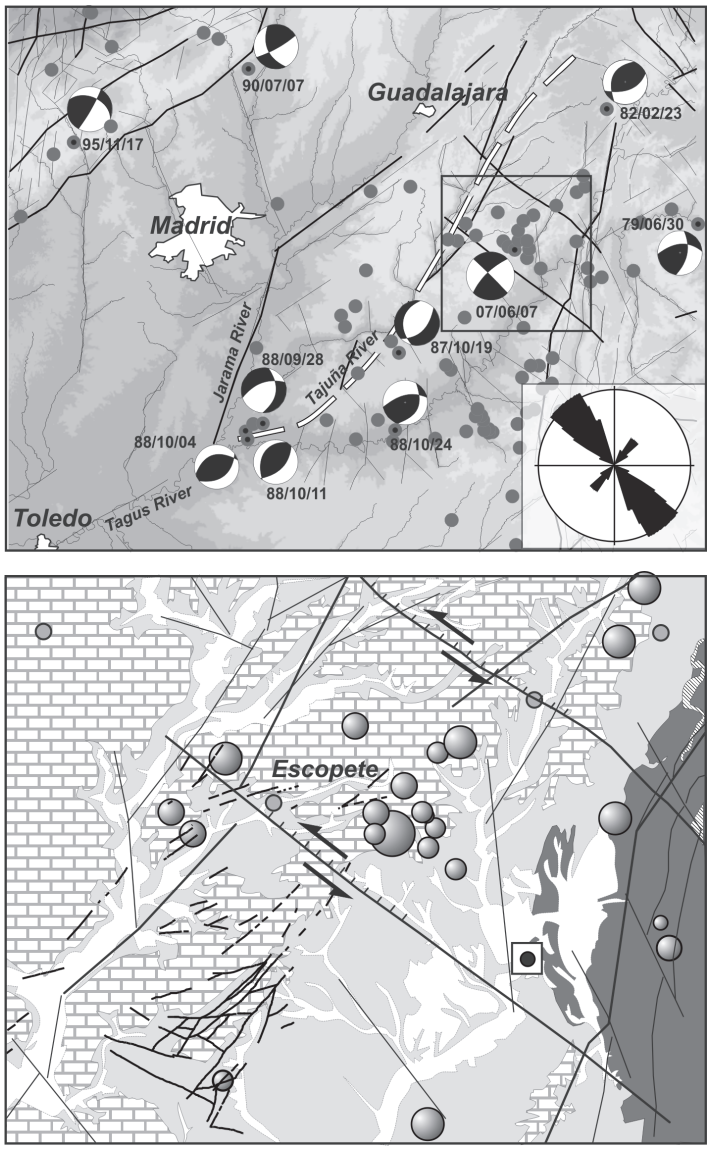

▲ **Figure 4.** Focal mechanisms of previous earthquakes in the region (Herráiz *et al.* 2000). Major faults extracted from Proyecto Prior (2007). The dashed line represents the axis of the cortical flexion interpreted by Giner-Robles (1996) and De Vicente *et al.* (2007). This regional flexure produces an extensional tectonic regime in the shallower areas of the crust that explains several normal fault extensional mechanisms (with a maximum horizontal shortening direction NE-SW). The direction rose shows the frequency of maximum horizontal shortening directions inferred from the analysis of focal mechanisms. The maximum oriented NE-SW trends correspond to extensional mechanisms. (B) Tectonic map of the epicentral area of the Escopete earthquake. Fault strikes taken from Muñoz-Martín and De Vicente (1998) and De Vicente *et al.* (2007).

Valley, 30 km to the east, where the first suburbs of the Madrid metropolitan area are located. The earthquake was widely reported in this area because of the higher population density.

The traditional architecture of the Alcarria region is mainly composed of loadbearing walls of fieldstone masonry set in weak mortar bonds. The towns of the area are therefore characterized by an aged building stock of high vulnerability, as can be seen from an analysis of the heritage town of Pastrana, the main town of the epicentral area with a population slightly greater than 1,000.

According to the 2001 census, Pastrana has a total of 879 buildings, 60% of which were built before 1900. We estimate that at least 70% of the buildings are of vulnerability A, and the remaining 30% are vulnerability B and C. We do not expect any buildings of lower vulnerability grades because of the area's low hazard, less than 0.04 g, which does not require the application of the Spanish seismic building code (NCSE-02).

The earthquake was widely felt in the epicentral area, where it woke up residents and set off car alarms. Seismic sounds were also reported throughout the epicentral area. There are a few isolated reports of objects falling from tables and shelves, although this does not appear to have been a generalized occurrence. There are also a few isolated reports of very slight damage, although no formal damage reports have been filed.

The maximum intensity of the earthquake appears to correspond closely to the description for intensity V EMS. However, the EMS-98 handbook states that intensity grades be seen as threshold values, which must be exceeded to be assigned that intensity. From this point of view, the available macroseismic information meets the conditions for intensity V in terms of effects on objects and people but appears to be insufficient in terms of damage reports. One would have expected more generalized cases of damage of grade 1 to confidently assign an intensity value of V. The intensity value assigned at the José Cabrera nuclear power plant, 9.2 km from the epicenter, was IV.

The earthquake's energy appears to have been channeled in a north-south direction, which may have been favored by the geological structures of the region and the earthquake's mechanism. The earthquake's perceptibility appears to have faded rapidly in an east-west direction, based on the lack of reports from the city center of Madrid, 60 km to the west of the epicenter. In contrast, there are felt reports from distant locations to the south (156 km) and to the north (220 km), which may represent the outer limits of the felt area for this event.

GROUND MOTION

Records and Derived Strong-motion Parameters

The earthquake was recorded at three strong-motion stations (GSR-16) located at the José Cabrera nuclear power plant (JCNPP), 9.2 km from the epicenter. The accelerometers (TERRA 16 bits) operate with a sample rate of 200 s/s. The stations are located in the electricity building (station CAB) and on free-field (stations RES and TOR).

Although the power plant is located along the alluvial terrace of the Tagus River, soil conditions at the station sites correspond to rock or firm soil. Stations CAB and RES are directly situated atop a 650-m-thick Tertiary substratum composed of evaporites, clay, and sandstones with average shear wave velocities of 1,300–1,500 m/s. The soil profile at station TOR is slightly different, because it includes Pliocene conglomerates in the uppermost 9 meters, with an average shear wave velocity of 500 m/s. According to the Eurocode 8 and National Earthquake Hazards Reduction Program (NEHRP) 2003 soil classifications, all stations are located on soil conditions B and A, respectively. Following the NCSE-02 soil classification, stations CAB and RES sites are at soil I conditions and station TOR is at soil II conditions. The characteristics of the soils at the three stations are summarized in Table 3.

The accelerograms were corrected for baseline errors and band-pass filtered between 0.2 and 0.4 Hz and 30 Hz. Some strong-motion parameters have been estimated and they are given in Table 4. In spite of the low magnitude of the earthquake, the motion had significant amplitude, mainly at stations CAB and RES. The recordings of these stations (maximum horizontal component) are shown in Figure 5.

Maximum recorded PGA values (horizontal components) range between 0.03 and 0.07 g (Table 4). These values exceed

TABLE 3
Soil Characteristics at the Strong-Motion Stations and Soil Categories According to Different Seismic Codes and Strong-Motion Models

Station	Location	Soil description	mean $v_{S,30}$	Soil class NCSE-02	Soil class EC-8
CAB	Electricity building	Rock	1300-1500 m/s	I	A
RES	Free field	Rock	1300-1500 m/s	I	A
TOR	Free field	Rock overlain by 9m of alluvial deposits	1060-1200 m/s	I	A

TABLE 4
Values Derived from the Records for Several Ground-Motion Parameters

Parameter	CAB			RES			TOR		
	NS	WE	V	NS	WE	V	NS	WE	V
PGA (g)	0.058	0.038	0.021	0.073	0.045	0.016	0.046	0.033	0.011
PGV (cm/s)	1.28	1.07	0.35	1.09	0.89	0.23	0.71	0.62	0.19
PGD (cm)	0.03	0.03	0.01	0.03	0.03	0.01	0.02	0.02	0.01
I Arias (cm/s)	0.79	0.70	0.23	1.42	0.63	0.10	0.35	0.25	0.07
CAV (cm/s)	41.38	41.78	27.27	52.56	36.69	20.15	25.75	24.73	16.33
$CAV_{stand.[25cm/s^2]}$ (cm/s)	14.90	15.63	0.00	22.00	12.49	0.00	9.69	7.98	0.00
Tp (s)	0.12	0.16	0.10	0.10	0.10	0.04	0.12	0.10	0.12
Significant duration (s)	2.72	3.66	4.39	2.23	3.29	6.11	2.20	3.24	6.10
Effective (s)	0.00	0.00	0.00	4.26	0.00	0.00	0.00	0.00	0.00
Epicentral distance	9,221m			9,558m			9,358m		
Azimut	128°32′21.3″			126°40′58.3″			126°31′17.8″		

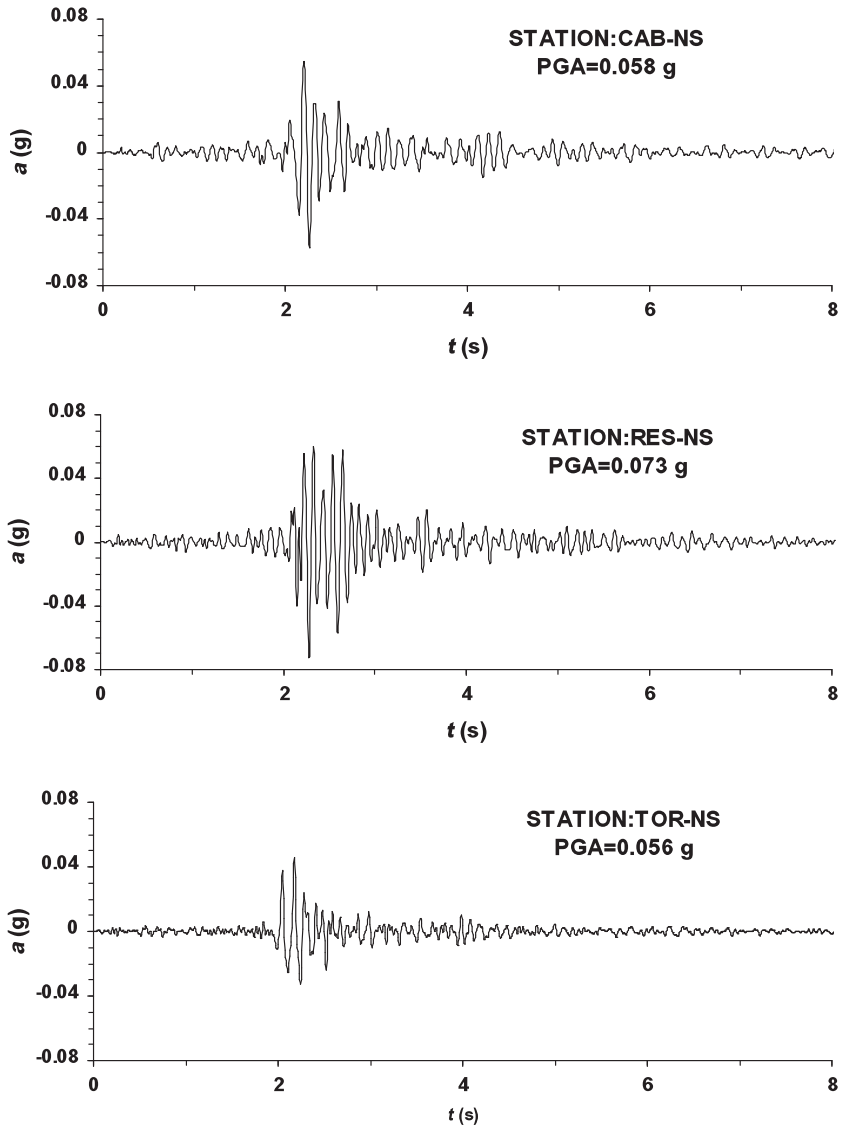

▲ **Figure 5.** Strong-motion records at the three stations located in the José Cabrera nuclear power plant (horizontal components with maximum PGA).

the value of a_b given by the hazard map of the Spanish seismic building code (NCSE-02) below 0.04 g for the central part of the Iberian peninsula (see Figure 2.).

The response spectra derived from the records have been compared with the ones predicted by some ground-motion models recently inferred from European data for a similar scenario: M_w= 4.2, epicentral distance R_{ep} = 9.2 km, and soil conditions matching those of our stations. The selected models are Berge-Thierry *et al.* 2003 (model B03), Ambraseys *et al.* 1996 (model A96), and Bommer *et al.* 2007 (model B07). Figure 6 shows the results of the comparison for the horizontal components at the three stations. Note in Figure 6A that *recorded* response spectra exceed the mean *predicted* response spectra for low periods (even for model B07, specifically developed from ground-motion data corresponding to small and moderate events). For longer periods (greater than 0.2 s), predicted spectra exceed the *recorded* ones. As Figure 6B illustrates, the recorded low-period ground motions can better be reproduced using the mean-plus-two-standard-deviations predicted response spectra. That means that the recorded spectra are close to the upper limit of the 95% confidence interval for short periods. The spectra derived from the records also exceed the ones derived from the codes for the short period range. Figure 6C contains the response spectra of Eurocode 8 (Comité Européen de Normalisation 2003) (Type 2, for **M** < 5.5) and of the NCSE-02, both scaled using a reference acceleration of 0.04 g (as the minimum a_b value of the NCSE-02 hazard map). The spectra derived from the records also exceed the ones derived from the codes.

A similar analysis has been carried out with other ground-motion parameters. The results are summarized in Table 4. We can see that Arias intensity (AI; Arias 1970) provides horizontal values between 0.35 and 1.42 cm/s. Expected values for a similar scenario are around 0.30–0.70 cm/s according to different authors (Cabañas *et al.* 1997; Sabetta and Pugliese 1996; Zonno and Montaldo 2002; Travasarou *et al.* 2003). Following these models, the recorded values are in the upper bound of the

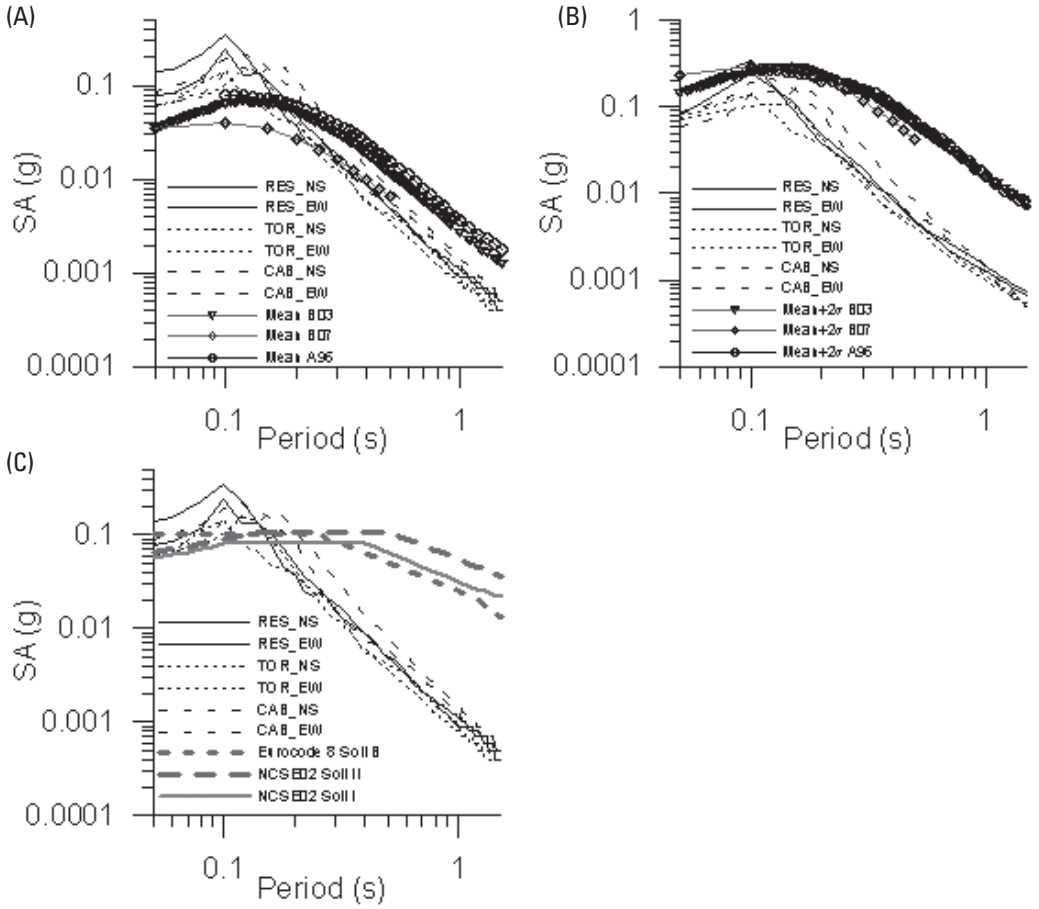

▲ **Figure 6.** Response spectra derived from the records for maximum horizontal components compared with: (A) the mean predicted by some strong-motion models inferred from European data for a similar scenario, (B) the upper limit of the 95% confidence interval predicted by the previous models, and (C) the response spectra of Eurocode 8 (Type 2, for **M** < 5.5) and NCSE-02 (scaled using a reference acceleration of 0.04 g).

expected values or even in excess of this limit for station RES (NS component).

The duration has been estimated according to two definitions: significant duration (Trifunac and Brady 1975) and effective duration (Bommer and Martínez-Periera 1999). The main difference is that the first takes the percent of IA (5% and 95%) and the second the absolute values of IA (1 cm/s and 12.5 cm/s) for truncating the record. We can see that with the relative criterion the significant duration arrives at values of 6.10 s, while with the absolute criterion the significant duration is null, with the exception of the strongest motion in RES (NS), which reaches a value of 4.26 s.

The analysis of the cumulative absolute velocity (CAV) and standardized CAV (with 25 cm/s^2 threshold, CAV_{25}) (Electric Power Research Institute 1988) requires special attention, since these parameters are used in the nuclear environment for establishing operating basis earthquake (OBE) exceedance criteria (together with the response spectra). Maximum CAV and CAV_{25} values derived from the records are 53 and 22 cm/s, respectively. This last parameter is high compared with the one given by Cabañas *et al.* (1997) for a similar scenario (between 4 and 14 cm/s), but is less than the value established for considering OBE exceedance, according to the criteria discussed in the next section.

To sum up, the strong-motion data available allows us to describe the ground motion produced by this earthquake as an impulsive motion, with relatively high PGA values and short-period spectral accelerations (around 0.1 s) and a very short (practically null) effective duration. Although no damage is reported, the NCSE-02 response spectra were exceeded for short periods.

Registered Motion Compared with the Strong-motion Parameters for Seismic Design of the José Cabrera Nuclear Power Plant

Our final analysis compares the ground-motion parameters derived from the records with the ones defined for the seismic design of the JCNPP.

The site under the JCNPP is seismically characterized by a response spectrum in free field and rock, corresponding to the safe shutdown earthquake (SSE), given by the spectral shape of U.S. Nuclear Regulatory Commission (USNRC) NUREG -0098 scaled by a PGA = 0.07 g in horizontal component and PGA = 0.046 g in vertical component (two-thirds of horizon-

tal PGA). The response spectra for the OBE is fixed as one-third of the spectrum of SSE, resulting in a value of PGA = 0.023 g. The instrumental criteria for considering exceedance of the OBE were taken from the USNRC Regulatory Guide 1.166 (USNRC 1997), which establishes the following conditions for JCNPP:

- The response spectra (acceleration or velocity) in horizontal or vertical components should be exceeded in certain given frequency ranges in RES.
- The CAV_{25} derived from the record of the station RES should exceed a value of 156.9 cm/s, (0.16 g.s).

In our case, the response spectra of the OBE have been exceeded by the registered ground motion in RES (horizontal and vertical components). However, the maximum value of CAV_{25} derived from the records is 22 cm/s, which is one order of magnitude less than the threshold value fixed for considering exceedance of the OBE (156.9 cm/s). The OBE was not exceeded according to these criteria.

SUMMARY OF MAIN RESULTS

This paper summarizes our in-depth study of the 7 June 2007 Escopete earthquake, located in the central part of the Iberian peninsula with magnitude mb_{Lg} 4.2, in a region traditionally considered stable with a very low level of seismicity. Historically, a few rare events have been felt in the region with intensity V (MKS), while the maximum recorded magnitude was 4.1. From the structural point of view, the area is characterized by significant tectonic activity from the middle Miocene to the Quaternary. The major deformation structures are coherent with a regional horizontal stress shortening direction NW-SE, which is consistent with the current convergence direction between the Iberian and African plates.

The earthquake was registered by 11 stations of the RSN with good azimuthal coverage, allowing us to obtain hypocentral parameters and focal mechanism solutions with a high degree of accuracy. The focus is located at 40.41° N, 2.98° W, with a depth of 6 km, near the town of Escopete. The moment tensor inversion reveals (as best solution) a strike-slip mechanism (azimuth = 225°, dip = 75°, slip = 179°), with fault planes oriented NNW-SSE and NE-SW and a scalar seismic moment of 3.1×10^{14} Nm.]This result also is supported by spectral analysis of *P* waves and is consistent with some NW-SE faults with sinistral strike-slip movements identified near the epicentral area.

In spite of its low magnitude, the earthquake was felt in an extensive area in the southern Alcarria region of the province of Guadalajara. The maximum intensity appears to correspond closely to the description for intensity V EMS-98. The earthquake's energy appears to have been channeled in a north–south direction, which may have been favored by the geological structures of the region and the earthquake's mechanism.

The region under study is of special interest due to the existence of two nuclear power plants: José Cabrera and Trillo. Three accelerometers installed in JCNPP recorded the ground motion for the Escopete earthquake and are the first such records from the central part of the Iberian peninsula. The PGA reached a value of 0.07 g, requiring attention from a seismic hazard point of view.

The hazard map of the Spanish seismic building code NCSE-02 establishes a basic acceleration a_b (corresponding to PGA in hard soil with a 10% exceedance probability in 50 years) of less than 0.04 g, which is the minimum value required for the application of the earthquake-resistant building code. However, the registered values are higher, a fact that may have implications for future revisions of the code.

The scarce strong-motion data available allows us to describe the ground motion produced by this earthquake as an impulsive motion with very short (practically null) effective duration and relatively high PGA values and short-period spectral accelerations (around 0.1 s) in comparison with the ones predicted (for a similar scenario) by different strong-motion models. Other ground-motion parameters, such as the Arias intensity and the bracketed cumulative absolute duration, reach values in the upper bounds given by the models.

The response spectra for the OBE of the Cabrera JCNPP (spectral shape of USNRC NUREG -0098 scaled by a PGA = 0.023 g) was also exceeded. Nevertheless, the maximum value of CAV_{25} derived from the records is 22 cm/s, which is one order of magnitude less than the threshold value fixed under this criterion (156.9 cm/s), so using this method, we cannot claim that the OBE has been exceeded.

Concluding Remarks

The central part of the Iberian peninsula, where the Escopete earthquake took place, is an example of a low seismic zone where infrequent earthquakes may generate ground motion higher than expected for a return period of 500 years. The occurrence of events such as the one studied in this paper suggests the need to develop studies aimed at a better understanding of the neotectonic activity, fault capacity, and maximum expected magnitudes for this area. The Escopete event seems tied to the activation of a secondary fault, raising the question of possible reactivation of other secondary faults in the area. Moreover, it is important to consider the possibility of a rupture in a main fault like the Altomira fault. This could cause a high-magnitude event consistent with the low *b*-value for the area. A thorough fault survey of the area would, therefore, be extremely useful.

The ground motion was recorded only by accelerometers of the JCNPP, since the IGN strong-motion network has no accelerometers in central Iberia. An array in Sonseca (Toledo) and other stations in San Pablo de los Montes (Toledo) are operating, but these are seismographs that provide only velocity records. To reduce the lack of detection in terms of acceleration, we should consider the deployment of strong-motion instruments in the region. Further monitoring would contribute to the study of energy-channelling effects, which seem evident from the observed intensity distribution of this event and other historical earthquakes.

The existence of two nuclear power plants and several dams, and the vulnerability of the structures and the proximity to large, populated areas, all support the need for further stud-

ies to better determine seismic risk. The information obtained from this and future events would be useful in drafting future codes for buildings and critical structures.

ACKNOWLEDGMENTS

UNIÓN FENOSA Generación is acknowledged for providing the strong-motion data used in this work. This work has been partly financed by the project AE10/07-15484 of the Universidad Complutense de Madrid and the projects RISTE CGL2006-10311-C03-01/BTE of the Ministerio de Educación y Ciencia.

REFERENCES

Ambraseys, N. N., K. A. Simpson, and J. J. Bommer (1996). Prediction of horizontal response spectra in Europe. *Earthquake Engineering and Structural Dynamics* **25**, 371–400.

Arias, A. (1970). A measure of earthquake intensity. In *Seismic Design for Nuclear Power Plants*, ed. R. J. Hansen, 438–483. Cambridge, MA: Massachusetts Institute of Technology Press.

Banda, E., E. Suriñach, A. Aparicio, J. Sierra, and E. Ruiz de la Parte (1981). Crust and upper mantle structure of the central Iberian meseta (Spain). *Geophysical Journal International* **67**, 779–789.

Berge-Thierry, C., F. Cotton, O. Scotti, D.-A Griot-Pommera, and Y. Fukushima (2003). New empirical response spectral attenuation laws for moderate European earthquakes. *Journal of Earthquake Engineering* **7** (2), 193–222.

Bommer, J. J., and A. Martínez-Periera (1999). The effective duration of earthquake strong motion. *Journal of Earthquake Engineering* **3** (2), 127–172.

Bommer, J. J., P. J. Stafford, J. E. Alarcón, and S. Akkar, S. (2007). The Influence of Magnitude Range on Empirical Ground-Motion Prediction. *Bulletin of the Seismological Society of America* **97**, 2,152–2,170.

Cabañas, L., B. Benito, and M. Herráiz (1997). An approach to the measurement of the potential structural damage of earthquake ground motions. *Earthquake Engineering and Structural Dynamics* **26**, 79–92.

Calvo, J. P., A. M. Alonso Zarza, M. A. García del Cura, S. Ordoñez, J. P. Rodríguez-Aranda, and M. E. Sanz-Moreno (1996). Sedimentary evolution of lake system through the Miocene of the Madrid basin: Paleoclimatic and paleohydrological constrains. In *Tertiary Basins of Spain*, ed. P. Friend and C. Dabrio, 272–277. Cambridge: Cambridge University Press.

Cesca, S., E. Buforn, and T. Dahm (2006). Amplitude spectra moment tensor inversion of shallow earthquakes in Spain. *Geophysical Journal International* **166** (2), 839–854; doi:10.1111/j.1365-246X.2006.03073.x.

Comité Européen de Normalisation (CEN) (2003). prEN 1998-1. *Eurocode 8: Design of Structures for Earthquake Resistance*. *Part 1: General Rules, Seismic Actions and Rules for Buildings*. Draft No 6, Doc CEN/TC250/SC8/N335, January 2003, Brussels.

DeMets, C., R. G. Gordon, D. F. Argus, and S. Stein (1990). Current plate motions. *Geophysical Journal International* **101**, 425–478.

DeMets, C., R. G. Gordon, D. F. Argus, and S. Stein (1994). Effect of recent revisions to the geomagnetic reversal time scale on estimate of current plate motions. *Geophysical Research Letters* **21**, 2,191–2,194.

De Vicente, G., R. Vegas, A. Muñoz-Martín, P. G. Silva, P. Andriessen, S. Cloetingh, J. M. González-Casado, J. D. Ven Wees, J. Álvarez, A. Carbó, and A. Olaiz (2007). Cenozoic thick-skinned deformation and topography evolution of the Spanish Central System. *Global and Planetary Change* **58**, 335–381.

Electric Power Research Institute (EPRI) (1988). *A Criterion for Determining the Exceedance of the Operating Basis Earthquake*. EPRI Report NP-5930. Palo Alto, CA: Electric Power Research Institute.

Giner, J. L., G. De Vicente, A. C. Pérez González, J. G. Sánchez Cabañero, and L. Pinilla (1996). Crisis tectónicas cuaternarias en la Cuenca de Madrid. *Geogaceta* **20** (4), 842–845.

Giner-Robles, J. L. (1996). Análisis geotectónico y sismotectónico en el sector centro-oriental de la Cuenca del Tajo. Tesis doctoral, Universidad Complutense de Madrid, 268 pps.

Herráiz, M., G. De Vicente, R. Lindo-Ñaupari, J. L. Giner-Robles, J. L. Simón, J. M. González-Casado, O. Vadillo, M. A. Rodríguez-Pascua, J. I. Cicuéndez, A. Casas, L. Cabañas, P. Rincón, A. L. Cortés, M. Ramírez, and M. Lucini (2000). A new perspective about the recent (Upper Miocene to Quaternary) and present tectonic stress distributions in the Iberian Peninsula. *Tectonics* **19** (4), 762–786.

Instituto Geográfico Nacional (IGN) (2007). Banco de datos sísmicos de la Red Sísmica Nacional [Spanish national seismic network].

Kiratzi, A., and C. B. Papazachos (1995). Active crustal deformation from the Azores triple junction to the Middle East. *Tectonophysics* **243**, 1–24.

Ligorría, J. P., and C. J. Ammon (1999). Iterative deconvolution and receiver function estimation. *Bulletin of the Seismological Society of America* **89** (5), 1,395–1,400.

Martínez Solares, J. M., and J. Mezcua (2002). *Catálogo sísmico de la Península Ibérica (880 a.C.–1900)*. Instituto Geográfico Nacional, Monografia 18.

McClusky, S., R. Reilinger, S. Mahmoud, D. Ben Sari, and A. Tealeb (2003). GPS constraints on Africa (Nubia) and Arabia plate motions. *Geophysical Journal International* **155**, 126–138.

Muñoz-Martín, A., and G. De Vicente (1998). Origen y relación entre las deformaciones y esfuerzos alpinos en la zona centro-oriental de la Península Ibérica. *Revista de la Sociedad Geológica de España* **11**, 57–70.

Norma de la Construcción Sismorresistente Española (NCSE-02) (2002). Real Decreto 997/2002, de 27 de septiembre, por el que se aprueba la norma de construcción sismorresistente: parte general y edificación (NCSE-02). *Boletín Oficial del Estado* **244**, 35,898–35,967.

Proyecto Prior (2007). Determinación de fallas de primer orden mediante el análisis integrado de datos geológicos. *Colección: Documentos I+D*. ISBN: 84-690-0234-1. Madrid: Consejo de Seguridad Nuclear, 312 pps.

Sabetta, F., and A. Pugliese (1996). Estimation of response spectra and simulation of nonstationary earthquake ground motions. *Bulletin of the Seismological Society of America* **86** (2), 337–352.

Travasarou, T., J. D. Bray, and N. A. Abrahamson (2003). Empirical attenuation relationship for Arias Intensity. *Earthquake Engineering and Structural Dynamics* **32**, 1,133–1,155.

Trifunac, M. D., and A. G. Brady (1975). A study on the duration of earthquake strong motion. *Bulletin of the Seismological Society of America* **65**, 581–626.

United States Nuclear Regulatory Commission (USNRC) (1997). *Regulatory Guide 1.166—Pre-Earthquake Planning and Immediate Nuclear Power Plant Operator Postearthquake Actions*. Washington, DC: USNRC.

Zonno, G., and V. Montaldo (2002). Analysis of strong ground motions to evaluate regional attenuation relationships. *Annals of Geophysics* **45**, 439–454.

Spanish Seismic Network
Instituto Geográfico Nacional
General Ibáñez Ibero, 3
28003-Madrid, Spain
echerrero@fomento.es
(E.C.H.)